Hindawi
International Journal of Photoenergy
Volume 2019, Article ID 1384985, 12 pages
https://doi.org/10.1155/2019/1384985

Research Article

An Advanced Multicarrier Residential Energy Hub System Based on Mixed Integer Linear Programming

Yue Yuan,[1] Angel A. Bayod-Rújula,[2] Huanxin Chen,[3] Amaya Martínez-Gracia,[4] Jiangyu Wang,[3] and Anna Pinnarelli[5]

[1]*China-Eu Institute for Clean and Renewable Energy, Huazhong University of Science and Technology, Wuhan 430074, China*
[2]*Department of Electrical Engineering, University of Zaragoza, Spain*
[3]*Department of Refrigeration & Cryogenics, Huazhong University of Science and Technology, 1037 Luoyu Road, 430074 Wuhan, China*
[4]*Department of Mechanical Engineering, University of Zaragoza, Spain*
[5]*Department of Mechanical, Energy and Management Engineering, University of Calabria, Arcavacata of Rende-Cosenza 87036, Italy*

Correspondence should be addressed to Angel A. Bayod-Rújula; aabayod@unizar.es

Received 27 February 2019; Accepted 14 May 2019; Published 9 June 2019

Academic Editor: Francesco Riganti-Fulginei

This work proposes a multicarrier energy hub system with the objective of minimizing the economy cost and the CO_2 emissions of a residential building without sacrificing the household comfort and increasing the exploitation of renewable energy in daily life. The energy hub combines the electrical grid and natural gas network, a gas boiler, a heat pump, a photovoltaic plant, and a photovoltaic/thermal (PV/T) system. In addition, to increase the overall performance of the system, a battery-based energy storage system is integrated. To evaluate the optimal capacity of each energy hub component, an optimization scheduling process and the optimization problem have been solved with the YALMIP platform in the MATLAB environment. The result showed that this advanced system not only can decrease the economic cost and CO_2 emissions but also reduce the impact to electrical grid.

1. Introduction

As the climate becomes increasingly polarized today, the demand for electricity and heating load of buildings also increases daily, sometimes even accounting for half of the total building energy consumption. Relying only on the electrical grid and natural gas network input to meet customer demand, energy utilization efficiency will be extremely low. Not only can the grid meet a huge pressure during peak load period, but it will also produce large amounts of CO_2 which will aggravate urban heat island effect, which makes the demand of polarization phenomenon more serious. In recent years, although renewable energy generation has been greatly developed, the constraint in terms of transport capacity of the electrical grid still becomes a bottleneck of its participation in energy supply. In last years, in order to provide a solution to these limits, a large number of small renewable energy generators have been connected to the distribution networks [1].

An energy hub is a multicarrier energy system consisting of multiple energy conversion, storage, and/or network technologies and is characterized by some degree of local control. Conception of an energy hub (EH) system has been first proposed on the research project "Vision of Future Energy Network" by ETH, Zurich, in 2007 [2]. In this future vision of energy networks, an energy hub system is a highly abstract unit structure, providing a great opportunity for system schedulers and operation workers to create a more efficient system [3]. An energy hub is an initial part of a multienergy

system, which can accommodate various forms of energy input and diversified load types [4]. Because of this diversified form of energy carrier, the energy hub system can realize collaborative optimization for various forms of energy [5]. In order to ensure that the energy hub is operated under a secure and economic and environmentally friendly condition, the research for energy hub systems mainly focuses on the component type or the capacity of an energy hub and the energy hub optimal dispatch [6–9]. Different from using traditional flat traffic, Le Blond et al. [10] introduced "dynamic traffic" to drive energy storage system operation to control energy hub system operation under minimum cost and CO_2 emissions. Beigvand et al. [11] proposed a new algorithm named SAL-TVAC-GSA to dispatch energy hub economic cost. In [9], Setlhaolo et al. present a residential energy hub model for a smart home as a modified framework of conventional energy hubs in a smart grid with consideration of heat pump water heater, coordination of sources, and carbon emission. Lingang Industrial Park is an engineering example [12], whose results provide a technical support for the construction of a resource-saving and environment-friendly harbour. In [13], a residential building and its electrical equipment are modelled as an energy hub system, including washing machine, dryer, HVAC system, refrigerator, and lighting equipment, to minimize energy cost, carbon emission, and peak load for optimal scheduling under the premise of maintaining the comfort of the users. In addition, a cloud computing framework is present to achieve the effective management of data and information. Ma et al. [8] presented a community micro energy grid in four different scenarios on a typical summer day, and the roles of renewable energy, energy storage devices, and demand response are discussed separately.

Due to the fact that an energy hub is an efficient means for the optimal exploitation of renewable energy generation, research focuses are generally concentrated on variable kinds of energy inputs [14–16]. Sharif et al. [17] presented a simulation model for an energy hub which major energy source is renewable energy (wind and solar energy) and natural gas. Ha et al. [18] proposed an energy hub system for residential buildings with solar energy and battery-based energy storage systems, and the results showed that this energy system structure conforms to the characteristics of residential buildings' energy consumption. Furthermore, it can reduce costs and save energy consumption at the same time. However, little research considers the integration of PV/T systems into an energy hub. PV/T can generate water heating and electricity at the same time [19], being an ideal component for residential energy hub system. This paper proposes a multicarrier energy hub (EH) system based on solar PV and PVT systems and a battery-based energy storage system. Moreover, an optimal scheduling strategy is proposed to calculate the optimum capacity of each component in order to minimize the energy cost and the CO_2 emission. The optimization problem has been solved with the YALMIP platform in the MATLAB environment. The proposed EH system is tested for a residential application according to the characteristics of buildings of apartments in Zaragoza, Spain.

2. Description of the Building Simulation Model and Optimization Process

A residential building located in Zaragoza, in the centre of Spain, with a simple but typical architecture as shown in Figure 1 has been simulated in EnergyPlus software. Climatic parameters, including ambient temperature, solar irradiation, and wind speed, have been taken from the Zaragoza local dataset. The simulation building is a 3-storey residential building, 1660.73 m^2, with five 3-bedroom apartments per floor. It has been considered that 4 people live in each apartment.

Solar irradiation in Zaragoza is abundant (see Figure 2), so it is reasonable to introduce photovoltaic (PV) systems or PV/T systems into energy hubs to decrease the energy costs and the CO_2 emissions.

The electricity price has been calculated from hourly local real-time price in Spain in 2017, as it is shown in Figure 3. The considered gas prices were 0.0667 euro/kWh and 0.0865 euro/kWh according to Spain gas prices for household consumers, all taxes and levies included in the first and second semester of 2017, respectively [20].

The daily energy consumption of the simulation building for four seasons is shown in Figure 4; blue bars represent electricity (including air conditioning) consumption and red curve represents heating demand (including heating and hot water demand). The highest electricity demand can approach 220 kWh per day (sum of the blue bar in Figure 4 for summer) and the highest heating demand is approximately 55 kWh per day (sum of grey values in Figure 4, winter).

Relying only on the electrical grid and natural gas network to satisfy electricity and heating demands of this building, the economic cost is 11713 euro/year and the CO_2 emission is 21711 kg/year (see Table 1).

An EH system has been so developed with the aim to minimize the energy cost and the CO_2 emissions but also for relief grid's pressure. Firstly, in accordance with the building's energy consumption pattern, an EH system with only a gas boiler (GB), a heat pump (HP), a PV plant (PV), and a PV/T system has been designed. A capital cost of 800 euro/kW has been considered for the GB and 1000 euro/kW for the HP, both with an estimated lifetime of 20 years. In the case of the PV plant, a capital cost of 1500 euro/kWp has been considered (including inverter, wire, and protections) and 700 euro/m^2 for the PVT systems and their lifetime has been considered to be 30 years. Later, the EH system has been improved with the integration of a BESS. The EH system design has been optimized by the optimization scheduling process as shown in Figure 5. The optimization problem is solved by using Mixed Integer Linear Programming (MILP) on the YALMIP platform in the MATLAB environment. Since there are too many elements included in the EH system, it is difficult to get the optimal solution directly through a single-layer optimization process. Therefore, the EH system design is threefold. Firstly, only the HP and the PV (with variable efficiency) are considered as elements involved in the operation of the EH system and for this configuration their optimum capacity is obtained. Then, operating the EH system under this optimum capacity, a PV/T (with variable

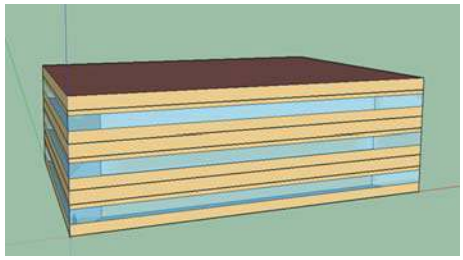

Figure 1: Building structure simulated in EnergyPlus software.

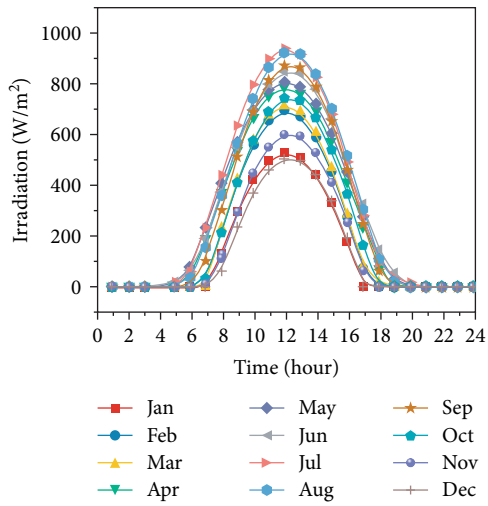

Figure 2: Average daily solar irradiation in Zaragoza for each month.

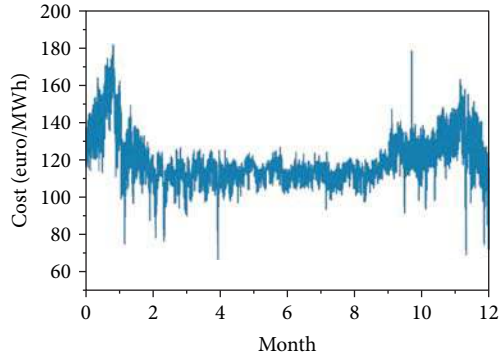

Figure 3: Actual hourly real-time electricity price in 2007.

thermal efficiency) is introduced into the EH system and the optimization schedule is solved again to calculate the optimal PV/T capacity. Finally, the BESS is integrated and the final optimal capacity of each element of the EH system is obtained. The entire process is modelled taking into account the dynamic price of electricity and natural gas.

The optimal operation model is formulated with the multiple objective of minimizing the entire cost, CO_2 emission, and peak load:

$$\begin{cases} \min \sum_{t-1}^{T-8760} \left[P_{\text{ele}}(t) p_{\text{ele}}(t) \Delta t + P_{\text{gas}}(t) \times p_{\text{gas}}(t) \Delta t \right] + F_{\text{install}} + f_{\text{O\&M}}, \\ \min \sum_{t-1}^{T-8760} P_{\text{ele}}(t) E_{\text{ele}}(t) \Delta t + \sum_{t-1}^{T} P_{\text{gas}}(t) E_{\text{gas}}(t) \Delta t, \\ \min P_{\text{ele}}^{\max}(t), \end{cases} \tag{1}$$

where $P_{\text{ele}}(t)$ and $P_{\text{gas}}(t)$ represent the price of electricity and gas from the main grid, respectively. $E_{\text{ele}}(t)$ and $E_{\text{gas}}(t)$ represent the CO_2 emission index of electricity and gas, respectively. F_{install} represents the installation fee of all components, and $F_{\text{O\&M}}$ represents the operation and management fee of all components.

Electricity balance constraints and heat balance constraints can be formulated as equations (2) and (4), respectively.

$$L_{\text{ele}}(t) = e_{\text{ele,grid}}(t) + e_{\text{ele,PV}}(t) + e_{\text{ele,PV/T}}(t) - e_{\text{ele,hp}}(t) - S_{\text{ele,B}}(t), \tag{2}$$

$$\begin{cases} e_{\text{ele,grid}}(t) = P_{\text{ele,grid}}(t) \eta_{\text{ele,grid}}(t), \\ e_{\text{ele,PV}}(t) = A_{\text{PV}} G(t) \eta_{\text{ele,PV}}(t), \\ e_{\text{ele,PV/T}}(t) = A_{\text{PV/T}} G(t) \eta_{\text{ele,PV/T}}(t), \end{cases} \tag{3}$$

where $e_{\text{ele,grid}}(t)$ is the electricity supplied from the main grid, $e_{\text{ele,PV}}(t)$ is the electricity supplied from the PV panel, and $e_{\text{ele,PV/T}}(t)$ is the electricity supplied from the PV/T panel; A_{PV} and $A_{\text{PV/T}}$ are the surface areas of the PV panel and the PV/T panels. $G(t)$ is the solar irradiance. $e_{\text{ele,hp}}(t)$ represents the electrical input of the heat pump at time, which is determined by heating balance constraints. And $S_{\text{ele,B}}(t)$ is the energy input or output from the battery.

$$L_{\text{heat}}(t) = h_{\text{heat,grid}}(t) + h_{\text{heat,PV/T}}(t) + h_{\text{ele,hp}}(t), \tag{4}$$

$$\begin{cases} h_{\text{heat,grid}}(t) = P_{\text{heat,grid}}(t) \eta_{\text{heat,grid}}(t), \\ h_{\text{heat,hp}}(t) = \text{COP}_{\text{hp}}(t) e_{\text{ele,hp}}(t), \end{cases} \tag{5}$$

where $h_{\text{heat,grid}}(t)$ and $h_{\text{heat,hp}}(t)$ represent the heating supplied from natural gas net and heat pump, respectively, and $h_{\text{heat,PV/T}}(t)$ is the heat supplied from the PV/T panel.

Solving the layer-by-layer optimization is helpful to know the impact of each element on the EH system and simplify the solving process at the same time. The building performance throughout the year is valuated with all the components at its optimum capacity.

3. The EH Structure and Matrix Representation

The first structure of the EH system proposed for the building is shown in Figure 6. Initially, a gas boiler (GB), a heat pump (HP), a PV plant (PV), and a PV/T system are considered besides the electrical grid and the natural gas network.

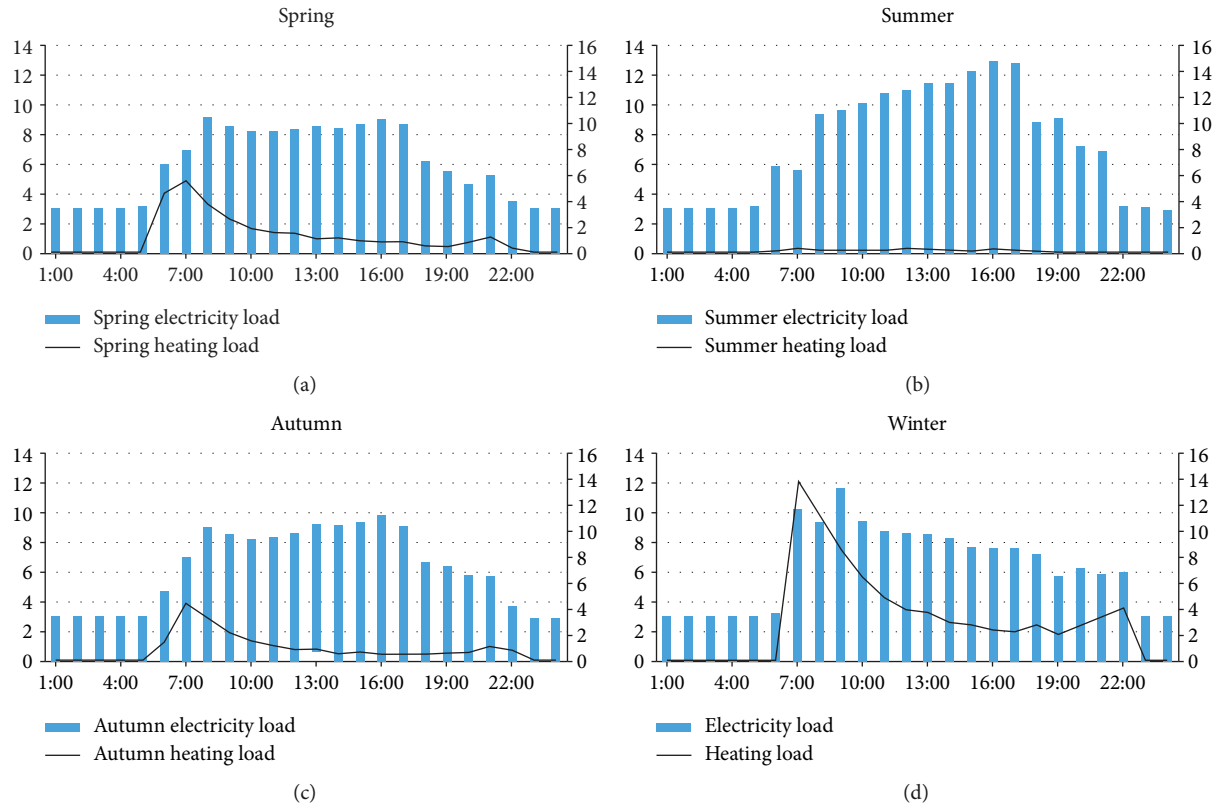

Figure 4: Daily energy consumption of the simulation building for different seasons.

Table 1: Cost, energy consumption, and CO_2 emissions for the traditional supply.

Cost (euro/year)	CO_2 emission (kg/year)	Gas consumption (kWh/year)	Electricity consumption (kWh/year)
11713	21711	20518	62589

The basic mathematical model of the EH system is [21]

$$L = f(P), \tag{6}$$

where L expresses the energy (electricity and heating) demand and considers the power supply.

The basic matrix function of the EH system can be written as

$$\begin{bmatrix} L_1 \\ L_2 \\ \vdots \\ L_n \end{bmatrix}_{n\times 1} = \begin{bmatrix} c_{11} & c_{12} \cdots c_{1m} \\ c_{21} & c_{22} \cdots c_{2m} \\ & \cdots \\ c_{n1} & c_{n2} \cdots c_{nm} \end{bmatrix}_{n\times m} \begin{bmatrix} P_1 \\ P_2 \\ \vdots \\ P_m \end{bmatrix}_{m\times 1}. \tag{7}$$

In this function, $c_{ij}{}^{\text{th}}$ is the coupling factor, which represents the conversion efficiency between the i^{th} energy input and the j^{th} energy output.

In this framework, the relationship between the demand side and the supply side of the EH system is formulated with a coupling matrix indicated as follows:

$$L = [C_1\ C_2] \begin{bmatrix} P \\ R \end{bmatrix}, \tag{8}$$

$$L = C_1 P + C_2 R. \tag{9}$$

Energy demand matrix L is equal to coupling matrix C times the installed generating capacity of P and the renewable energy R.

$C_1 P$ can be developed as

$$C_1 P = \begin{bmatrix} \eta_{\text{grid}} & \eta_{\text{heatpump}} & \eta_{\text{boiler}} \end{bmatrix} \begin{bmatrix} P_{\text{grid}} \\ P_{\text{heatpump}} \\ P_{\text{boiler}} \end{bmatrix}, \tag{10}$$

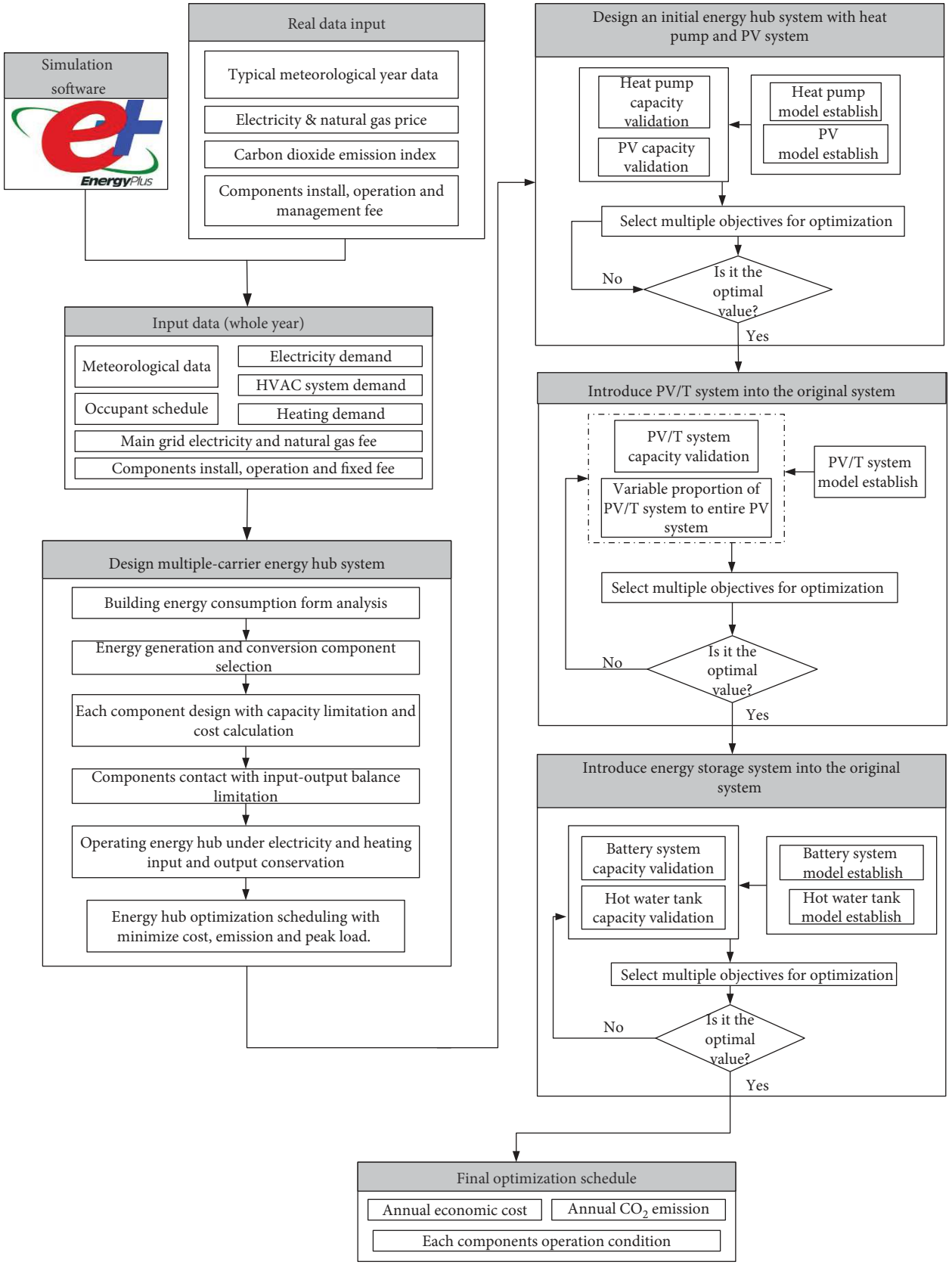

Figure 5: EH system optimization scheduling process.

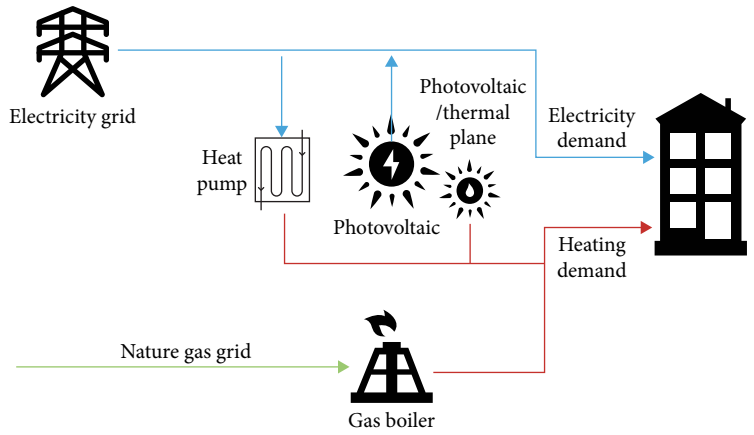

Figure 6: EH system structure for the building.

$$C_1P = \left[\eta_{\text{grid}}P_{\text{grid}} + \eta_{\text{heatpump}}P_{\text{heatpump}} + \eta_{\text{boiler}}P_{\text{boiler}}\right], \quad (11)$$

$$\begin{cases} \eta_{\text{grid}}P_{\text{grid}} = \begin{bmatrix} \eta_{\text{grid,ele}} \\ \eta_{\text{grid,heat}} \end{bmatrix} \begin{bmatrix} P_{\text{grid,ele}} \\ P_{\text{grid,heat}} \end{bmatrix}, \\ \eta_{\text{heatpump}}P_{\text{heatpump}} = \begin{bmatrix} \eta_{\text{heatpump,ele}} \\ \eta_{\text{heatpump,heat}} \end{bmatrix} \begin{bmatrix} P_{\text{heatpump,ele}} \\ P_{\text{heatpump,heat}} \end{bmatrix}, \\ \eta_{\text{boiler}}P_{\text{boiler}} = \begin{bmatrix} \eta_{\text{boiler,ele}} \\ \eta_{\text{boiler,heat}} \end{bmatrix} \begin{bmatrix} P_{\text{boiler,ele}} \\ P_{\text{boiler,heat}} \end{bmatrix}. \end{cases} \quad (12)$$

In (7), due to the value of $\eta_{\text{boiler,ele}}P_{\text{boiler,ele}}$ which is equal to 0, the equation can be represented as

$$C_1P = \begin{bmatrix} \eta_{\text{grid,ele}}P_{\text{grid,ele}} + \eta_{\text{heatpump,ele}}P_{\text{heatpump,ele}} \\ \eta_{\text{grid,heat}}P_{\text{grid,heat}} + \eta_{\text{heatpump,heat}}P_{\text{heatpump,heat}} + \eta_{\text{boiler,heat}}P_{\text{boiler,heat}} \end{bmatrix}. \quad (13)$$

C_2R can be represented as

$$C_2R = \begin{bmatrix} \eta_{\text{PV}} \\ \eta_{\text{PV/T}} \end{bmatrix} \begin{bmatrix} P_{\text{PV}} \\ P_{\text{PV/T}} \end{bmatrix}, \quad (14)$$

$$C_2R = \begin{bmatrix} \eta_{\text{PV,ele}}P_{\text{PV,ele}} + \eta_{\text{PV/T,ele}}P_{\text{PV/T,ele}} \\ \eta_{\text{PV,heat}}P_{\text{PV,heat}} + \eta_{\text{PV/T,heat}}P_{\text{PV/T,heat}} \end{bmatrix}. \quad (15)$$

Because the value of $\eta_{\text{PV,heat}}P_{\text{PV,heat}}$ is equal to 0, C_2R can be represented as

$$C_2R = \begin{bmatrix} \eta_{\text{PV,ele}}P_{\text{PV,ele}} + \eta_{\text{PV/T,ele}}P_{\text{PV/T,ele}} \\ \eta_{\text{PV/T,heat}}P_{\text{PV/T,heat}} \end{bmatrix}. \quad (16)$$

For each EH system component, the following parameters are included: capacity, efficiency, capital cost, fixed cost, variable cost, and lifetime as reported in Table 2. The electricity net emission factor considered is 0.28 kg/kWh and 0.204 kg/kWh for natural gas [22].

In real-life application, the PV efficiency is not a constant value; it varies with such parameters as solar irradiation, environmental temperature, and PV panel surface temperature. The working temperature of the cells (T_c) depends exclusively on the solar irradiation G and the ambient temperature (T_a) according to the linear function

$$T_c - T_a = C_2G, \quad (17)$$

where C_2 is represented by

$$C_2 = \frac{\text{NOCT}(^\circ\text{C}) - 20}{800\ \text{W/m}^2}. \quad (18)$$

NOCT in equation (18) is the nominal operating cell temperature defined as the temperature reached by open circuited cells in a module under 800 W/m^2 cell surface irradiance and ambient temperature of 20°C and so on. NOCT of a typical commercial module is approximately 45 ± 2°C, accordingly, C_2 is approximately equal to 0.3°C/(W/m^2).

Therefore, if the PV nominal power value under STC condition (P_n) is known, it will be possible to figure out the PV power value at any time via

$$P_m = P_n\frac{G}{G_{\text{STC}}}[1 - \gamma(T_c - 25)], \quad (19)$$

where G_{STC} is the irradiation under standard test conditions (STC), which is equal to 1000 W/m^2.

In a conventional PV plant of crystalline silicon, the conversion efficiency is in the range 15%-20% so 75% to 80% of the solar energy is not being used effectively [22]. Besides, the unused solar energy will heat up the panel, causing a decrease in the efficiency of the electricity generation.

Transferring the thermal energy to a heat transfer fluid, we obtain useful thermal energy and refrigerate the photovoltaic cells at the same time. This system, which can make use of solar light and thermal simultaneously, is called photovoltaic/thermal integrated system (PV/T system) (Figure 7).

Table 2: EH system component parameters.

Component name	Efficiency (%)	Capital cost (€/kW or €/m^2)	Fixed cost (€/kW)	Variable cost (€/kWh)	Lifetime (years)
Gas boiler	70	800	10	0.02	20
Heat pump	3.2 (COP)	1000	8.7	0	20
PV	Variable	250	2	0	30
PV/T	Variable	700	10	0	30

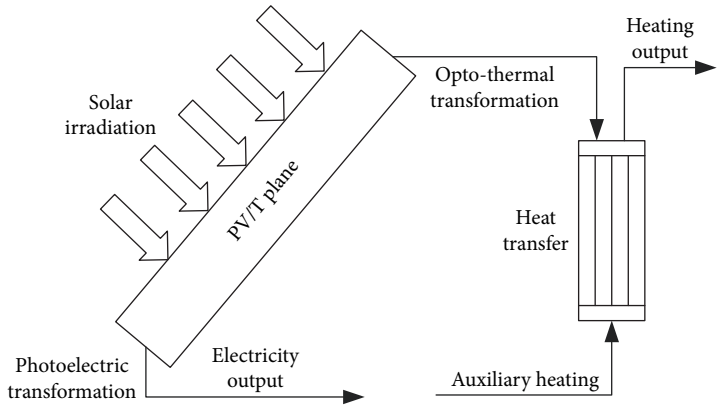

Figure 7: The schematic of the PV/T system.

The calculation about the thermal part of the PV/T system is shown as follows:

$$Q_S = G \times A_C, \tag{20}$$

$$Q_C = \eta_h \times Q_S, \tag{21}$$

$$Q_C = \text{cpw} \times \text{mw}_\text{C} \times (t_{\text{we\_c}} - t_{\text{ws\_c}}), \tag{22}$$

$$Q_d = A_C \times U_d \times (t_{\text{we\_c}} - t_0), \tag{23}$$

$$Q_{\text{cons}} = \text{cpw} \times m_r \times \left(t_{\text{d\_ini}} - t_{\text{pipe}}\right), \tag{24}$$

$$\begin{aligned} \int_0^{\text{inct}} (Q_C - Q_d - Q_{\text{cons}}) &= \text{cpw} \times \text{mw}_\text{d} \times (t_{\text{d\_fin}} - t_{\text{d\_ini}}) \\ &= \text{cpw} \times m_r \times \left(t_{\text{consig}} - t_{\text{d\_fin}}\right). \end{aligned} \tag{25}$$

Q_S represents the radiation projected onto the PV plane, Q_C is the heat absorbed by the panel, η_h is the heating efficiency of the PV/T systems, mw_C is the fluid mass under the panel, $t_{\text{we\_c}}$ and $t_{\text{ws\_c}}$ are output and input temperature of under panel fluid, respectively, Q_d is the heat loss of natural convection heat transfer between the tube and the environment, and t_0 represents the ambient temperature. Q_{cons} refers to the heat loss of direct heat transfer between the fluid in the pipe and the pipe wall. $t_{\text{d\_ini}}$ and $t_{\text{d\_fin}}$ are fluid input and output pipe temperature, respectively. t_{pipe} is the temperature of pipe shall and t_{consig} is the final demand fluid temperature. Q_a is the auxiliary energy supply. The thermodynamic relationship characterizing the PV/T is shown in Figure 8.

In addition, the thermal part of the PV/T system efficiency η_h is influenced by many factors, such as solar irradiation and pipe fluid temperature, as represented in

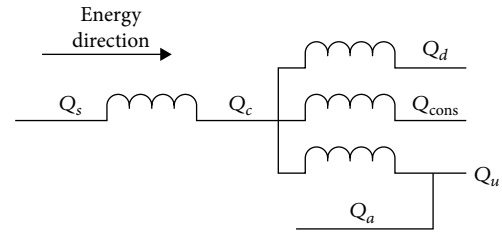

Figure 8: Thermodynamic relationship in the PV/T systems.

$$\eta_h = \eta_0 - a_1 \times \frac{(T_e - T_a)}{G} - a_2 \times \frac{(T_e - T_a)}{G}. \tag{26}$$

In this equation, η_0 means the optical performance of the PV/T system, a_1 and a_2 are the thermal loss coefficients, in this paper set as 3.3 (W/m^2)/K and 0.018 (W/m^2)/K^2, respectively, and I represents solar irradiation. T_e is the average value of pipe fluid temperature and T_a is the ambient temperature.

First of all, the scale of the PV/T system water tank is shown in Table 3.

$$V_d = \pi \left(\frac{D_d}{2}\right)^2 H_d, \tag{27}$$

$$A_d = 2\pi \left(\frac{D_d}{2}\right)^2 + \pi D_d H_d. \tag{28}$$

The temperature of the PV and PV/T panels is shown in Figure 9. Obviously, the PV/T surface temperature is higher

Table 3: Hot water tank dimension.

Name	Signal	Value	Unit
Tank volume	V_d	0.326	m^3
Panel surface area	A_c	3.26	m^2
Tank height	H_d	0.744	m
Tank bottom diameter	D_d	0.744	m
Tank surface area	A_d	5.22	m^2

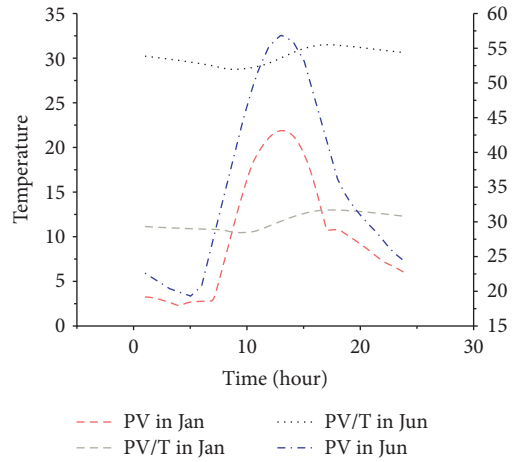

Figure 9: Panel temperature comparison between the PV and PV/T systems.

than the PV panel in summer season. In order to decrease the PV/T surface temperature, the hot water tank size should be enlarged. In this case, the hot water tank size is related to panel area, when V_d/A_c value is increased from 0.1 to 0.2, the hot water tank will become bigger gradually. Figure 9 presents the panel temperatures for $V_d/A_c = 0.2$.

The thermal efficiency of the PV/T system is shown in Figure 10.

The average daily electricity generation for 1 m^2 PV and PV/T panel with an 18% efficiency is shown in Figure 11 for every month. A PV/T system can generate more electricity in winter months and part of spring and autumn.

4. Energy Hub Results

The optimum values of the EH system components' capacity for the building under analysis were calculated in a previous paper [22] for a 20 kW HP and 65 m^2 of PV systems. With the combination of PV+PVT, the best results were obtained for a HP of 20 kW, 36 m^2 of PV modules, and 30 m^2 of PV/T. With the operating condition of 20 kW HP and 65 m^2 of PV systems, the cost reaches the minimum value 10727 euro/year. The CO_2 emission achieved 13560 kg/year at the meantime. Comparing these values with the total supply of electricity and heat from the electrical grid and natural gas network, respectively (see Table 1), a reduction of 8.42% in cost was obtained with a reduction of 37.54% in CO_2 emission. Otherwise, the results considering the optimal capacity of PV/T and PV systems (36 m^2 of PV and 30 m^2 of PV/T) are shown in Table 4. Compared with the result shown in Table 1, a great improvement is reached. A decrease of 10.61% in cost with a reduction of 30.02% in electricity consumption and 60.07% in gas consumption is achieved. A reduction of 39.66% in CO_2 emissions is also obtained.

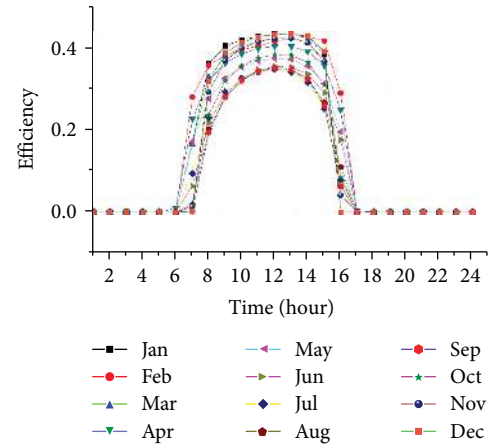

Figure 10: Daily efficiency for different months.

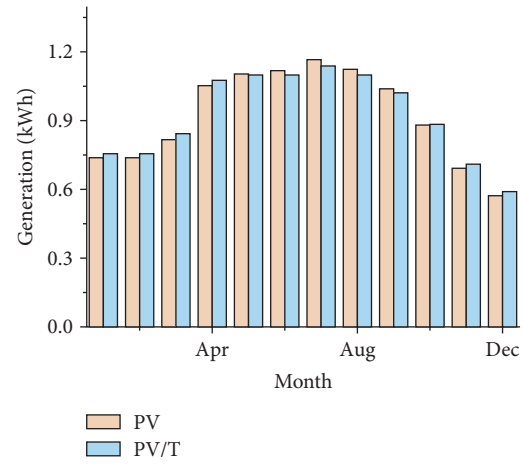

Figure 11: Average daily electricity generation for 1 m^2 of PV and PV/T panel for every month.

Table 4: Cost, electricity and gas consumption, and CO_2 emissions for the optimal sizing (20 kW of HP, 36 m^2 of PV, and 30 m^2 of PV/T).

Cost (euro/year)	Electricity consumption (kWh/year)	Gas consumption (kWh/year)	CO_2 emission (kg/year)
10470	43800	4419	13100

5. Energy Hub with a Battery-Based ESS

The renewable generation is sometimes greater than customer's demand and part of electricity generated from a

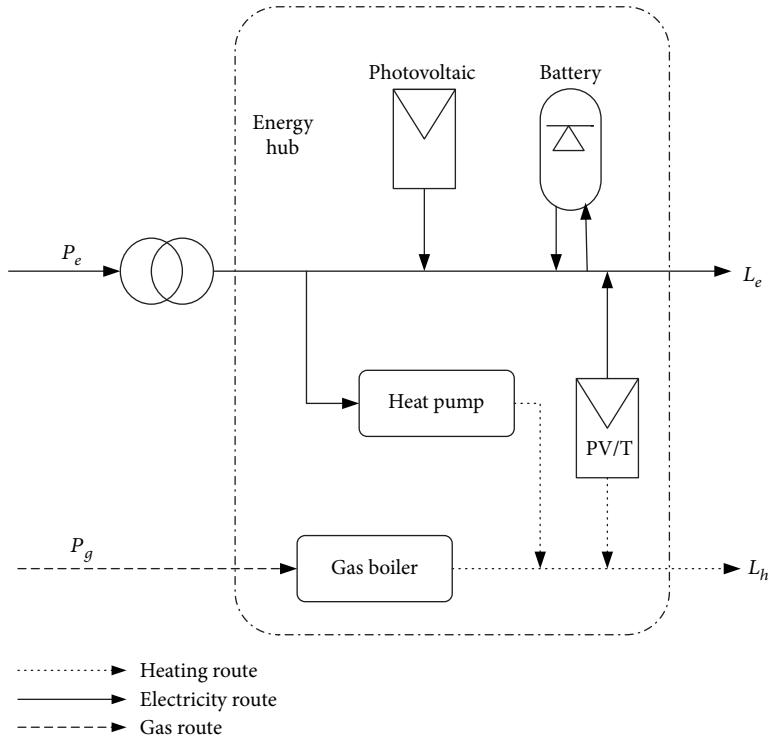

Figure 12: Ultimate energy hub structure for a building.

Table 5: Advanced EH system performance for several BESS sizes.

Battery capacity (kWh)	Cost (euro/year)	Electricity consumption (kWh/year)	CO_2 emission (kWh/year)
1	10211	41690	12520
2	10205	41650	12510
3	10200	41620	12500
4	10195	41590	12500
5	10190	41560	12490
6	10185	41530	12480
7	10179	41500	12470
10	10165	41410	12450
12	10214	41340	12430
15	10230	41280	12410

PV plant must be injected into the electrical grid or wasted. In order to improve the EH system performance, a BESS is integrated. The BESS provides a solution in case the renewable energy cannot be injected due to the regulation code (zero-injection schemes) or due to technical restrictions at that time. It is even able to provide voltage and frequency support and contribute to demand response procedures such as peak shaving. So, the advanced EH system structure is shown in Figure 12 with the BESS integrated.

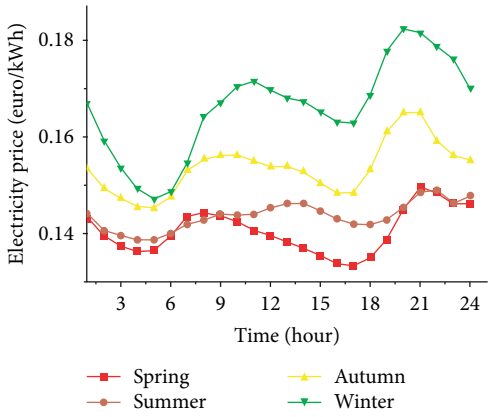

Figure 13: Daily electricity price for different seasons.

In this work, the battery is optimally charged and discharged to compensate the generation fluctuation of the PV and PV/T. The BESS dynamic model used is

$$E \times \mathrm{SOC}_t = E \times \mathrm{SOC}_0 + t_s \sum_{\gamma=1}^{t} \left\{ \eta_c P_{b,\gamma} - \frac{\bar{P}_{b,\gamma}}{\eta_d} \right\}, \quad 1 \le t \le N. \tag{29}$$

E is the BESS capacity, SOC_0 is the initial SOC of the BESS, SOC_t is the SOC at the given time t, $P_{b,\gamma}$ and $\bar{P}_{b,\gamma}$ are the continuous variables at time step γ, and $t_s \sum_{\gamma=1}^{t} \eta_c P_{b,\gamma}$

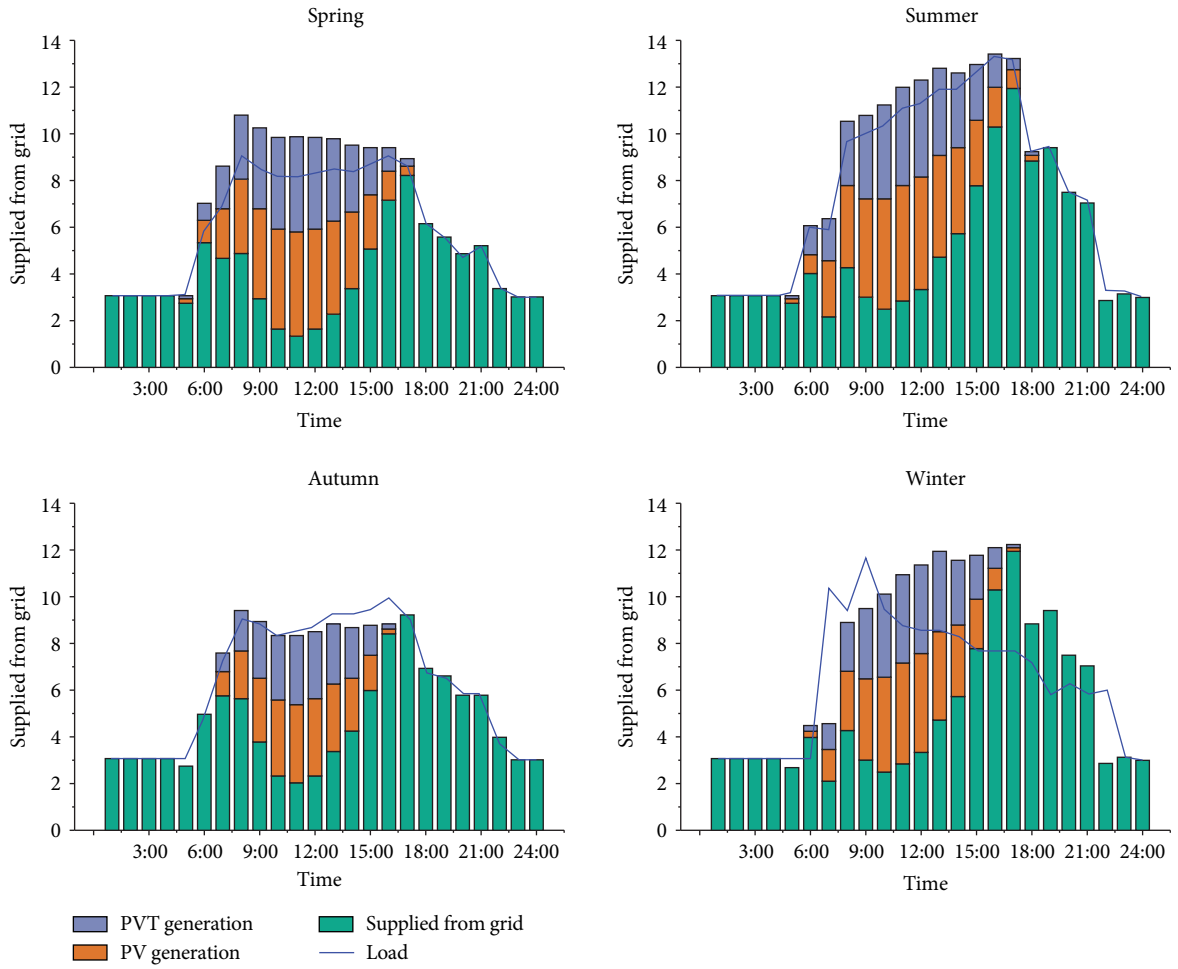

Figure 14: Energy structure in the proposed energy hub for different days of the four seasons.

and $t_s\sum_{\gamma=1}^{t}(\bar{P}_{b,\gamma}/\eta_d)$ are the BESS energy during the charging and discharging period, respectively.

BESS constraints are applied to the model:

$$0.2 \le SOC_t \le 0.8, \quad t = 1, \cdots, N, \tag{30}$$

$$P_{b,t} \times \bar{P}_{b,t} = 0, \quad t = 1, \cdots, N. \tag{31}$$

N is the number of sampling intervals; in this case, it is 8760.

The capacity limits are given in equations (30) and (31), which does not allow the BESS to charge and discharge at the same time. This constraint also permits the idle state of BESS.

The BESS involved here is an ideal model, which has a linear charge state and a SOC around 0.2 to 0.8. The optimization objective of BESS is the same as the previous system, minimum cost and minimum CO_2 emission. Due to the economic goal of the whole system, the BESS will be charged during the low electricity price period, and when the electricity price is high, it will discharge energy to satisfy the demand.

Now the matrix of this advanced EH system is shown as follows; S is the storage coupling matrix and E is the storage energy.

$$L = C_1 P + C_2 R - SE. \tag{32}$$

Table 5 shows the results of the simulation for different sizes of battery. The lowest cost is obtained for a battery of 10 kWh of capacity. Comparing with the results of Table 4, 2.91% cost and 5.46% CO_2 emission will be saved. Comparing with the results of Tables 1, 13% cost, 42.7% CO_2 emission, and 33.8% will be saved. Therefore, the simulation results confirm that adopting the proposed advanced EH system and the related optimization scheduling process not only significantly promotes efficiency and cost savings but also provides relief from the global pressure of greenhouse effect.

Four representative days for the four seasons of the year have been selected. Daily electricity prices for these days are presented in Figure 13. In Figure 14, the energy absorbed from PV, PV/T, and electrical grid for these representative days is shown.

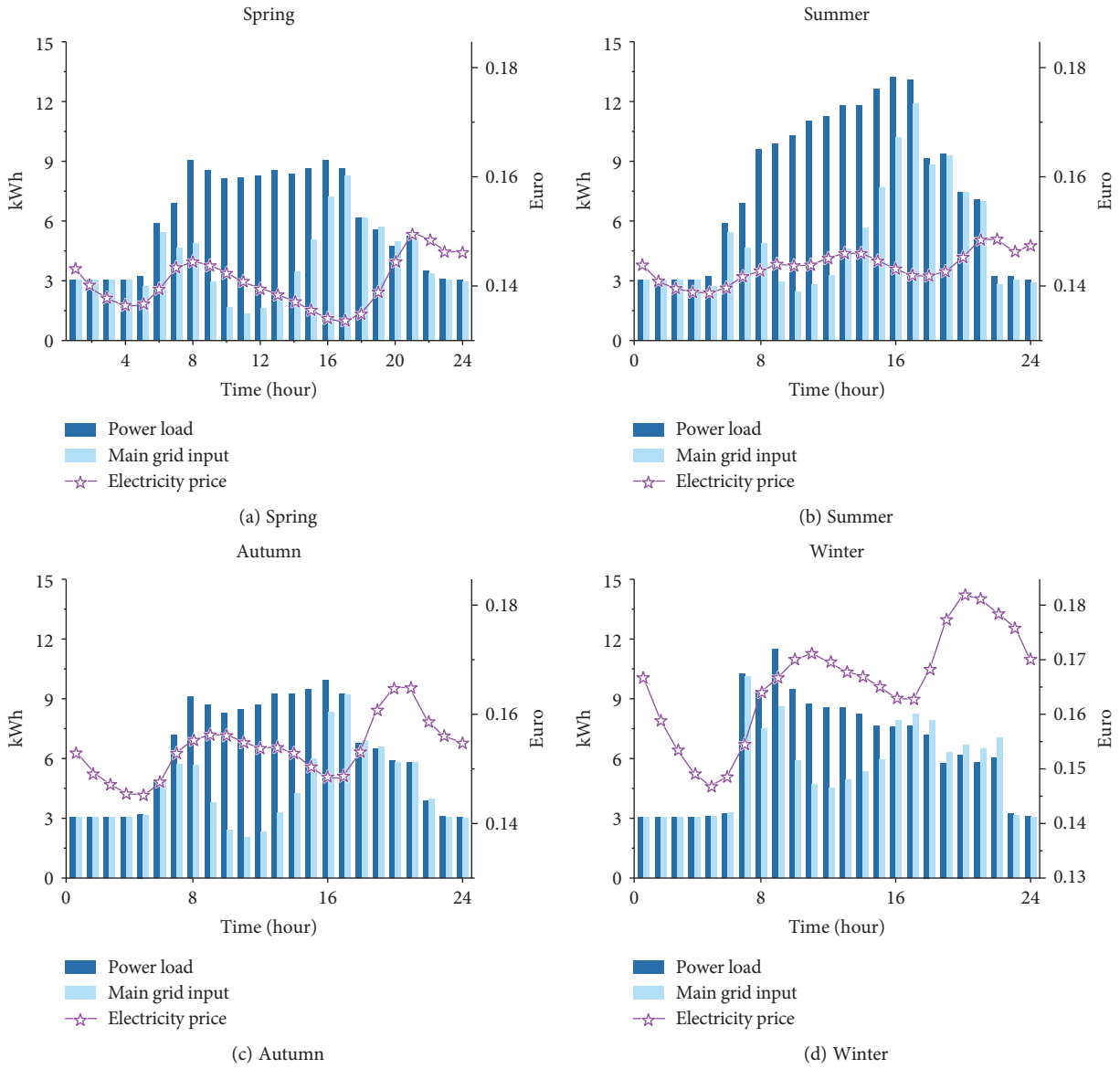

Figure 15: Comparison between electrical grid supply without the EH system and with the advanced EH system for different representative days for the four seasons.

Sometimes the supply is not totally equal to the demand due to the presence of BESS. When electricity price is high, the EH system avoids the supply of electricity from the electrical grid. In Figure 14, it is easy to find out that the EH system generates more electricity than the demand in autumn and winter which is related to the fact that electricity price is higher in these two seasons; indeed, the EH system chooses discharging via BESS to meet the customers' demand.

During the high demand hours, the EH system showed an outstanding performance for reduction of the absorption of energy from the electrical grid (Figure 15). Calculating according to that high demand hours from 8:00 a.m. to 16:00 p.m., the EH system can reduce 65.3%, 61.6%, 57.9%, and 33.9% absorption from the electrical grid. Meanwhile, during this period, 6.21 euro, 7.95 euro, 6.37 euro, and 4.14 euro are saved per day, respectively, for this building. Besides, due to the function of BESS, the electrical grid will supply more electricity when the price is relatively low.

6. Conclusions

This paper proposes an advanced multicarrier energy hub integrating not only generation components such as PV and PV/T systems but also a battery-based energy storage system to improve the performance. The optimal capacity of each component of the multicarrier energy hub in order to minimize the energy cost and the CO_2 emissions is based on the use of an optimization scheduling process solved on the YALMIP platform in the MATLAB environment. The simulation results confirm that large-scale utilization of the proposed approach will lead to significant cost and CO_2 savings.

Data Availability

The data used to support the findings of this study are included within the article.

Conflicts of Interest

The authors declare that there is no conflict of interest regarding the publication of this paper.

Acknowledgments

The authors gratefully acknowledge the support of National Natural Science Foundation of China (Grant 51876070) and (Grant 51576074).

References

[1] A. A. Bayod-Rújula, "Future development of the electricity systems with distributed generation," *Energy*, vol. 34, no. 3, pp. 377–383, 2009.

[2] H. X. Zhao and F. Magoulès, "A review on the prediction of building energy consumption," *Renewable and Sustainable Energy Reviews*, vol. 16, no. 6, pp. 3586–3592, 2012.

[3] P. Favre-Perrod, "A vision of future energy networks," in *Power engineering society inaugural conference and exposition in Africa*, pp. 13–17, Durban, South Africa, 2006.

[4] G. T. Ayele, P. Haurant, B. Laumert, and B. Lacarrière, "An extended energy hub approach for load flow analysis of highly coupled district energy networks: illustration with electricity and heating," *Applied Energy*, vol. 212, pp. 850–867, 2018.

[5] P. Cui, J. Shi, F. Wen et al., "Optimal energy hub configuration considering integrated demand response," *Dianli Zidonghua Shebei/Electric Power Automation Equipment*, vol. 37, pp. 101–109, 2017.

[6] M. Moeini-Aghtaie, A. Abbaspour, M. Fotuhi-Firuzabad, and E. Hajipour, "A decomposed solution to multiple-energy carriers optimal power flow," *IEEE Transactions on Power Systems*, vol. 29, no. 2, pp. 707–716, 2014.

[7] A. Sheikhi, M. Rayati, S. Bahrami, and A. Mohammad Ranjbar, "Integrated demand side management game in smart energy hubs," *IEEE Transactions on Smart Grid*, vol. 6, no. 2, pp. 675–683, 2015.

[8] T. Ma, J. Wu, and L. Hao, "Energy flow modeling and optimal operation analysis of the micro energy grid based on energy hub," *Energy Conversion and Management*, vol. 133, pp. 292–306, 2017.

[9] D. Setlhaolo, S. Sichilalu, and J. Zhang, "Residential load management in an energy hub with heat pump water heater," *Applied Energy*, vol. 208, pp. 551–560, 2017.

[10] S. Le Blond, R. Li, F. Li, and Z. Wang, "Cost and emission savings from the deployment of variable electricity tariffs and advanced domestic energy hub storage management," in *2014 IEEE Pes General Meeting | Conference & Exposition*, pp. 1–5, National Harbor, MD, USA, July 2014.

[11] S. D. Beigvand, H. Abdi, and M. La Scala, "A general model for energy hub economic dispatch," *Applied Energy*, vol. 190, pp. 1090–1111, 2017.

[12] X. Tian and R. Zhao, "Energy network flow model and optimization based on energy hub for big harbor industrial park," *Journal of Coastal Research*, vol. 73, pp. 298–303, 2015.

[13] M. C. Bozchalui, S. A. Hashmi, H. Hassen, C. A. Canizares, and K. Bhattacharya, "Optimal operation of residential energy hubs in smart grids," *IEEE Transactions on Smart Grid*, vol. 3, no. 4, pp. 1755–1766, 2012.

[14] M. Rastegar and M. Fotuhi-Firuzabad, "Load management in a residential energy hub with renewable distributed energy resources," *Energy and Buildings*, vol. 107, pp. 234–242, 2015.

[15] K. Orehounig, R. Evins, V. Dorer, and J. Carmeliet, "Assessment of renewable energy integration for a village using the energy hub concept," *Energy Procedia*, vol. 57, pp. 940–949, 2014.

[16] M. Sepponen and I. Heimonen, "Business concepts for districts' energy hub systems with maximised share of renewable energy," *Energy and Buildings*, vol. 124, pp. 273–280, 2016.

[17] A. Sharif, A. Almansoori, M. Fowler, A. Elkamel, and K. Alrafea, "Design of an energy hub based on natural gas and renewable energy sources," *International Journal of Energy Research*, vol. 38, no. 3, pp. 363–373, 2014.

[18] T. Ha, Y. Zhang, V. V. Thang, and J. Huang, "Energy hub modeling to minimize residential energy costs considering solar energy and BESS," *Journal of Modern Power Systems and Clean Energy*, vol. 5, no. 3, pp. 389–399, 2017.

[19] P. G. Charalambous, G. G. Maidment, S. A. Kalogirou, and K. Yiakoumetti, "Photovoltaic thermal (PV/T) collectors: a review," *Applied Thermal Engineering*, vol. 27, no. 2-3, pp. 275–286, 2007.

[20] Eurostat, https://ec.europa.eu/eurostat/statistics-explained/index.php/Natural_gas_price_statistics#Natural_gas_prices_for_household_consumers.

[21] A. Parisio, C. del Vecchio, and A. Vaccaro, "A robust optimization approach to energy hub management," *International Journal of Electrical Power & Energy Systems*, vol. 42, no. 1, pp. 98–104, 2012.

[22] A. A. Bayod-Rújula, Y. Yuan, A. Martínez-Gracia, J. Wang, J. Uche, and H. Chen, "Modelling and simulation of a building energy hub," *Proceedings*, vol. 2, no. 23, article 1431, 2018.